Acyl Transfer from Phosphocholine Lipids to Melittin: Electronic Supplementary Information

Catherine J. Pridmore,[a] Jackie A. Mosely,[a] Alison Rodger[b] and John M. Sanderson*[a]

Materials and Methods

Synthetic melittin (>97% by HPLC) was Alexis brand from Enzo Life Sciences (Exeter, UK). Stock solutions of melittin in water were prepared and used fresh. The melittin concentration of the stock solution (typically ~0.4 mM) was determined by absorbtion measurements at 280 nm after dilution of small aliquots into water (the extinction coefficient was calculated as 5500 M^{-1} cm^{-1}).[1] 1,2-Dioleoyl-*sn*-glycero-3-phosphocholine (DOPC), 1-oleoyl-*sn*-glycero-3-phosphocholine (1-oleoyl-PC), 2,5-dihydroxybenzoic acid (DHB) and α-cyano-4-hydroxycinnamic acid (CHA) were purchased from Sigma-Aldrich, Dorset, UK. 1-palmitolyl-2-oleoyl-*sn*-glycero-3-phosphocholine (POPC) was obtained from Avanti Polar Lipids *via* Instruchemie B.V., The Netherlands.

Liposomes were prepared by concentrating a solution of the lipid (typically 165 μl of a 2 mg/ml solution in $CHCl_3$) *in vacuo* to form a thin film on the side of a round bottomed flask. The lipid film was hydrated with 1 ml of aqueous medium containing 150 mM NaCl buffered with 10 mM sodium phosphate at pH 7 and mixed thoroughly before being subjected to five freeze thaw cycles and extruded 10 times through 100 nm laser-etched polycarbonate membranes (Whatman) at 30 °C using a thermobarrel extruder (Northern Lipids, Burnaby, Canada).

In a typical experiment, the melittin stock solution (32.5 μl, 1.3×10^{-8} mol) was added to the liposome preparation (150 μl, 6.3×10^{-8} mol) to give a mixture with final melittin and lipid concentrations of 71 μM and 0.35 mM respectively. The pH values of the solution (pH 7) was unchanged after mixing. The mixture was incubated at 37 °C for the remainder of the experiment.

For TLC analyses of lipid mixtures (*e.g.* Fig. S1), a portion (30 μl) of the mixture was removed and lyophilised. The residue was treated with $CHCl_3$/MeOH (1:1, 30 μl) and 15 μl of this solution spotted on the TLC plate. Chromatograms for *lyso*-PC analysis were developed on aluminium-backed Merck silica gel 60 plates using $CHCl_3$/MeOH/H_2O (6:4:1) and stained by dipping in a 10% *w*/*v* solution of phosphomolybdic acid in EtOH, followed by the application of heat. In order to quantify spot intensities, the TLC plate was scanned and the colour table of the image inverted using ImageJ (U. S. National Institutes of Health, Bethesda, Maryland, USA, version 1.44e) before being converted to greyscale. The pixel intensity (grey value) was measured and the baseline of the profile corrected to give the experimental profile. The experimental profile for each spot was modeled using a Gaussian function. For TLC analyses of melittin (*e.g.* Fig. S4), a portion (6 μl in 2 μl portions) of the melittin/lipid mixture was spotted directly onto a TLC plate. Chromatograms were developed using $CHCl_3$/MeOH/H_2O (6:4:1) and stained initially with 0.03% *w*/*v* Coomassie brilliant blue in 20% *v*/*v* MeOH/H_2O for 20 min, and then destained for 5 min in 20% *v*/*v* MeOH/H_2O, before drying under a stream of warm air (from a heat gun). Secondary staining was connducted on these plates by dipping them in a 5% *w*/*v* solution of ninhydrin in EtOH and then heating at 100 °C (on a hotplate).

MALDI-MS analyses were conducted on an Ultraflex II MALDI-TOF/TOF spectrometer with 337 nm nitrogen laser (Bruker Daltonics Ltd., Coventry, UK). Positive ion MS analyses were made using the reflectron. Positive ion MS/MS experiments were made using the LIFT capability in the absence of a collision gas and at a source pressure of 2.5×10^{-7} mBar. Data were analysed with Flex Analysis version 3.0 and Biotools version 3.0 (Bruker Daltonics Ltd). An aliquot of the melittin-lipid mixture (9 μl) was mixed with a solution of CHA (20 mg/ml in 30:70 (*v*/*v*) MeCN/H_2O + 0.1% TFA, 10 μl) and 1 μl applied to a ground steel target plate (cleaned with methanol and acetone before use) and allowed to air dry. MS analyses in the mass region of melittin were calibrated with the sodium adducts of poly(propylene glycol) 3000. For measurements of *lyso*-PC peak intensities, an aliquot of the lipid mixture (1 μl) was mixed with a solution of DHB (30 mg/ml in 50% *v*/*v* EtOH/H_2O, 9 μl) before spotting 1 μl on the target plate and allowing to air dry.

In the case of MS/MS spectra, base peak normalisation was performed. For measurement on *lyso*-PC formation, the *lyso*-PC peak intensities were normalised according to Eq. S1,

$$I_N = \frac{(I^H_{lyso} + I^{Na}_{lyso})}{(I^H_{lyso} + I^{Na}_{lyso} + I^H_{PC} + I^{Na}_{PC})} \quad \text{(S1)}$$

where

I_N is the normalised intensity,

I^H_{lyso} is the intensity of the protonated *lyso*-PC peak,

I^{Na}_{lyso} is the intensity of the sodiated *lyso*-PC peak,

I^H_{PC} is the intensity of the protonated PC peak and

I^{Na}_{PC} is the intensity of the sodiated PC peak.

MS data were acquired in an automated fashion. The laser power was varied over a very narrow limits, starting from the threshold of ion detection and controlled using fuzzy logic. A total of 500 spectra were averaged, collected from 20 positions per sample spot with 25 laser shots per position.

Thin Layer Chromatography (TLC)

Fig. S1 shows a TLC chromatogram of a sample of the melittin-DOPC mixture, following concentration by lyophilisation and dissolution of the residue in $CHCl_3$/MeOH.

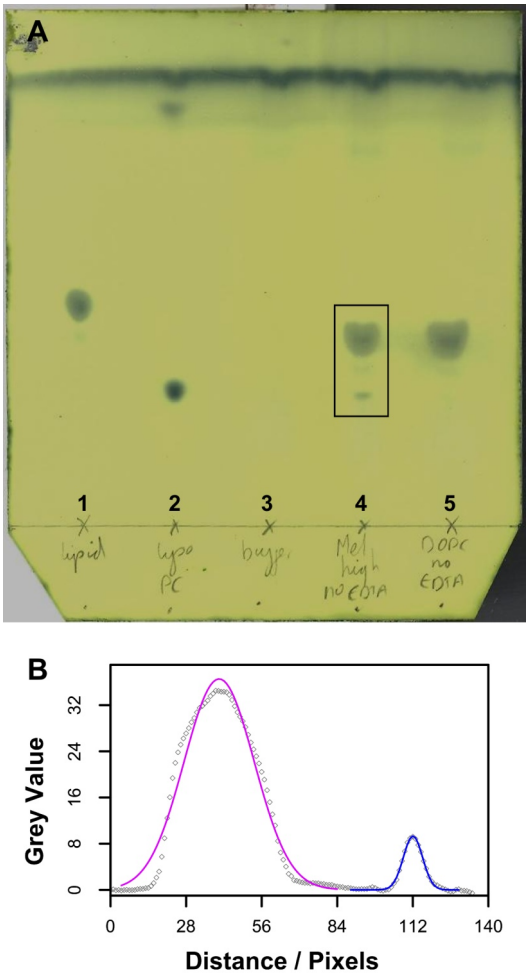

Fig. S1 (A) TLC analysis of an aliquot (15 µl) from a mixture of melittin and DOPC after 17 h, following lyophilisation and dissolution of the residue in $CHCl_3$/MeOH. The rectangle indicates the region of the plot used to generate the profile in Fig. S1B. Lanes are as follows: 1, DOPC (spotted from $CHCl_3$); 2, 1-oleoyl-PC (spotted from $CHCl_3$); 3, empty; 4, DOPC liposomes + melittin; 5, DOPC liposomes. (B) Pixel intensity profile across the DOPC and *lyso*-PC spots (points). The solid lines are Gaussian curves fit to the spot profiles by least squares methods.

Analysis of the *lyso*-PC and DOPC spot intensities following colour table inversion gave the profiles shown in Fig. S1B. Ftting of the peaks to Gaussian functions gave peak areas of 83 grey units.pixel and 1170 grey units.pixel for the *lyso*-PC and DOPC spots repsectively, a ratio of 1:14. In order to estimate the quantity of *lyso*-PC in the sample in molar terms, it was necessary to account for any differences in the ability of PMA to stain DOPC and *lyso*-PC. Therefore, chromatograms with known quantities of 1-oleoyl-PC and DOPC were run in order to compare the relative staining ability (Fig. S2).

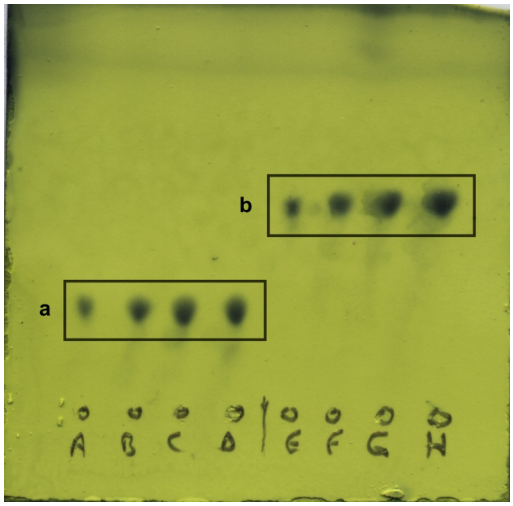

Fig. S2 1-Oleoyl-PC and DOPC standards. Lanes (A) to (D) correspond respectively to 0.17, 0.34, 0.51 and 0.68 µg 1-oleoyl-PC; lanes (E) to (H) correspond respectively to 0.2, 0.4, 0.6, 0.8 µg DOPC. The two boxes (a and b) correspond to the regions used for determining pixel intensity profiles.

From the gradients of the two plots in Fig. S3C and Fig S3D, it was apparent that PMA was 0.6 times as effective at staining *lyso*-PC than DOPC. This factor of 0.6 was used in calculation of the relative amounts of *lyso*-PC and DOPC from the sample in Fig. S1.

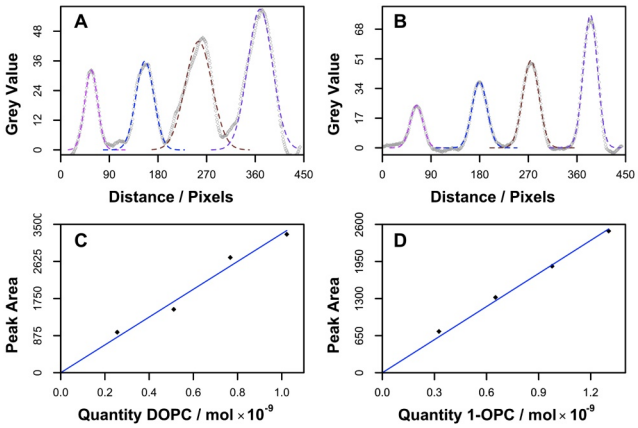

Fig. S3 Pixel intensity profiles across the DOPC (A) and 1-oleoyl-PC (B) TLC spots from Fig. S2 (regions b and a respectively). The dashed lines are Gaussian curves fit to the spot profiles by least squares methods. (C) and (D) show the variation of peak area as a function of the quantity of lipid spotted on the plate. The gradients of linear fits to the data are 3.3×10^{12} and 1.9×10^{12} grey units.pixel mol^{-1} for (C) and (D) respectively.

Complete conversion of melittin to oleoyl-melittin would lead to the formation of one equivalent of *lyso*-PC, and given the initial peptide:lipid ratio of 1:5, this would be equivalent to a molar *lyso*-PC:DOPC ratio of 1:4 and a corresponding ratio of TLC spot intensities of 1:7 after correction. Assuming that there was no additional formation of *lyso*-PC by hydrolysis, the extent of conversion of melittin to oleoyl-melittin from the observed ratio of spot intensities (1:14) in Fig. S1 could therefore be estimated as 50 ± 10%.

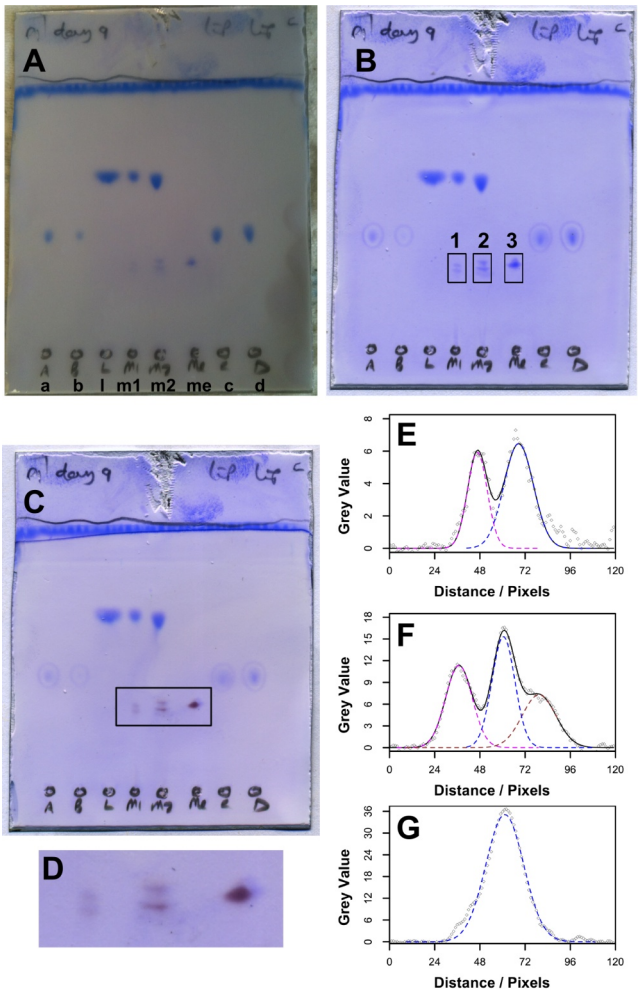

Fig. S4 TLC analysis of a sample of melittin (71 μM) and POPC (0.35 mM) following incubation at 37 °C in PBS for 9 days. In (A) to (C), lanes 'a', 'b', 'c' and 'd' correspond respectively to 0.17, 0.34, 0.51 and 0.68 μg 1-oleoyl-PC (spotted from 10% MeOH/$CHCl_3$), lane 'l' is 6 μl of the liposome control (without melittin) spotted directly onto the plate, lane 'm1' is 2 μl of the melittin-lipid mixture spotted directly onto the plate, lane 'm2' is 6 μl of the melittin-lipid mixture spotted directly onto the plate and lane 'me' is a stock solution if melittin in PBS (without lipid) spotted directly onto the plate. The plate was developed in $CHCl_3$/MeOH/H_2O (6:4:1) and stained initially with Coomassie brilliant blue (0.03% *w*/*v* in 20% *v*/*v* MeOH/H_2O; 20 min at room temperature followed by 5 min destain in 20% *v*/*v* MeOH/H_2O). (A) shows the plate immediately after destaining (before drying). (B) shows the plate after drying and (C) shows the plate after secondary staining with a 5% *w*/*v* solution of ninhydrin in EtOH (with heating at 100 °C for 1 min). (D) shows an enlarged view of the boxed region in (C). (E), (F) and (G) are profile plots of regions 1, 2 and 3 respectively in part (B).

A key feature of Fig. S4 is the presence of two spots that stain well with both Coomassie blue and ninhydrin, suggesting the presence of at least two distinct peptide products. Migration of melittin in these chromatograms was entirely dependent on the presence of salt (melittin spotted from water remained on the baseline), but nevertheless, melittin spotted from PBS gave single spot that could be well fitted by a Gaussian function, in contrast to the lipid samples.

POPC Kinetic Profile

Fig. S5 shows the kinetic profile for the reaction between melittin and POPC at 37 °C, pH 7.

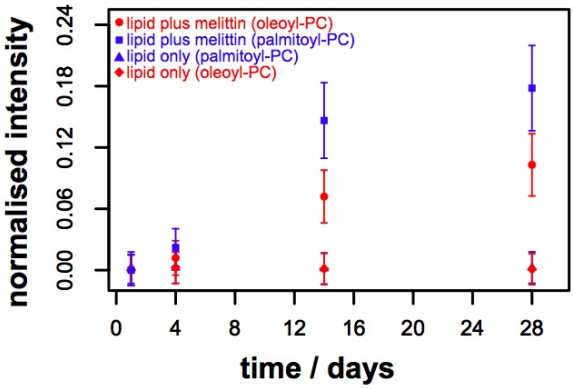

Fig. S5 The formation of *lyso*-PC monitored by MALDI-MS following mixing of melittin (71 μM) with POPC liposomes (0.35 mM) in PBS at 37 °C and pH 7. MALDI-MS was performed using 2,5-dihydroxybenzoic acid as matrix. Normalised *lyso*-PC peak intensities were calculated according to Eq. S1. Errors are estimated from repeat MS experiments.

1-oleoyl-PC/DOPC Calibration Curve

A series of standard mixtures with known concentrations of 1-oleoyl-PC and DOPC were prepared in PBS and analysed by MALDI-MS using DHB as matrix under the same conditions as the experiments with melittin. A calibration curve showing the normalised relative intensity of 1-oleoyl-PC peaks as a function of the mole fraction of 1-oleoyl-PC in the mixture (Fig. S6) was then constructed.

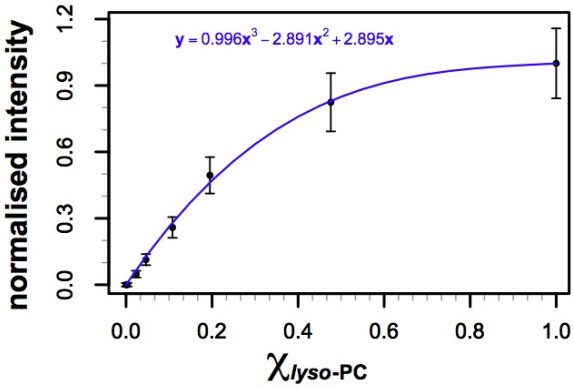

Fig. S6 Variation of normalised 1-oleoyl-PC peak intensities in mass spectra of mixtures of 1-oleoyl-PC with DOPC in response to changes in the mole fraction ($\chi_{lyso\text{-}PC}$) of 1-oleoyl-PC. Normalised intensities were calculated according to Eq. S1. Experimental values are represented as points and the best 3rd order polynomial fit to these data as a line.

The experimental value for the normalised intensity of oleoyl-PC peaks at the end of the experiment with melittin and DOPC was 0.3 ± 0.05, which corresponds to an oleoyl-PC mole fraction of 0.1 ± 0.02. Complete conversion of melittin to oleoyl-melittin would give a oleoyl-PC mole fraction of 0.2. The extent of melittin conversion to oleoyl-melittin can therefore be estimated at 50 ± 10%.

Overview of the Acylation Reaction

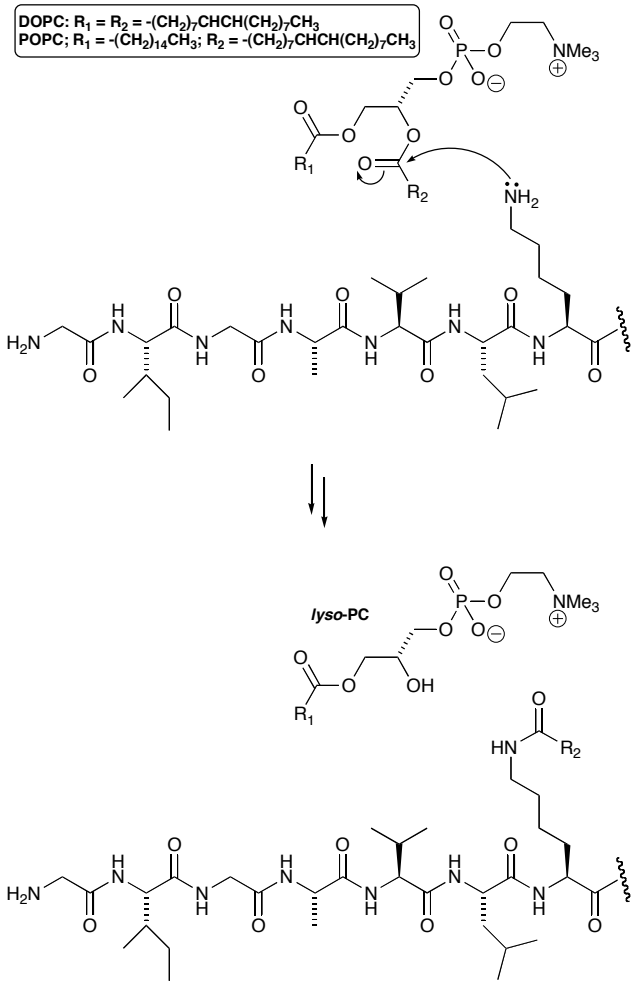

Fig. S7 Partial mechanism for the reaction of melittin with POPC and DOPC. The example shown is for reaction between the side chain of K7 and the *sn*-2 acyl group.

MS/MS Data

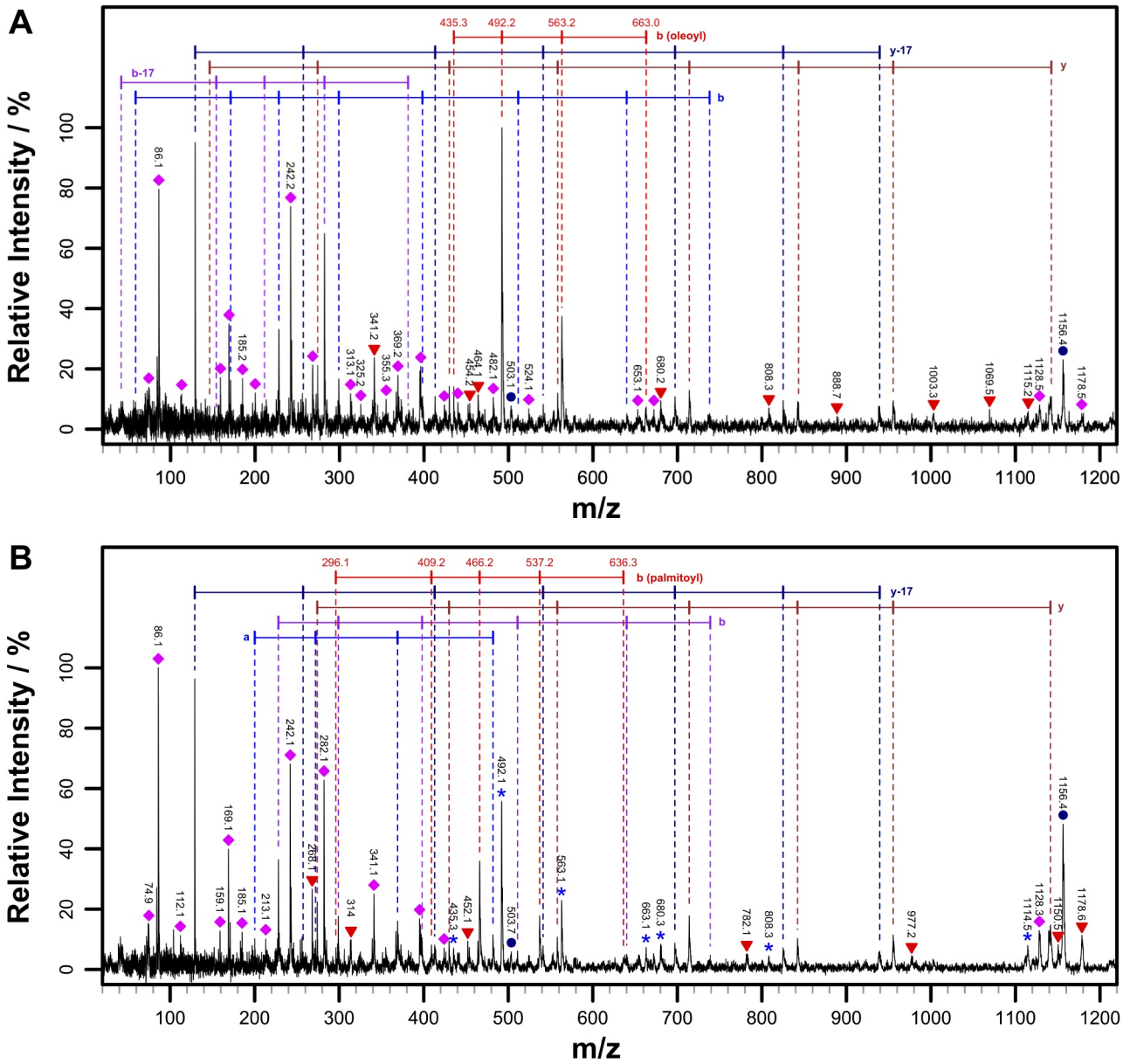

Fig. S8 Low mass region of the MS/MS fragmentation spectra of (A) oleoyl-melittin (*m/z* 3110) and (B) palmitoyl-melittin (*m/z* 3083). Dashed vertical lines correspond to ion series, with the ion type denoted for each at the top of the spectrum. Product ions that correspond to potential matches for modified fragments are indicated by triangles. Product ions that correspond to unmodified fragments are indicated by diamonds. Unidentified peaks are indicated by circles. Asterisks denote product ions arising from incomplete isolation of the parent ion. For full peak listings *vide infra*.

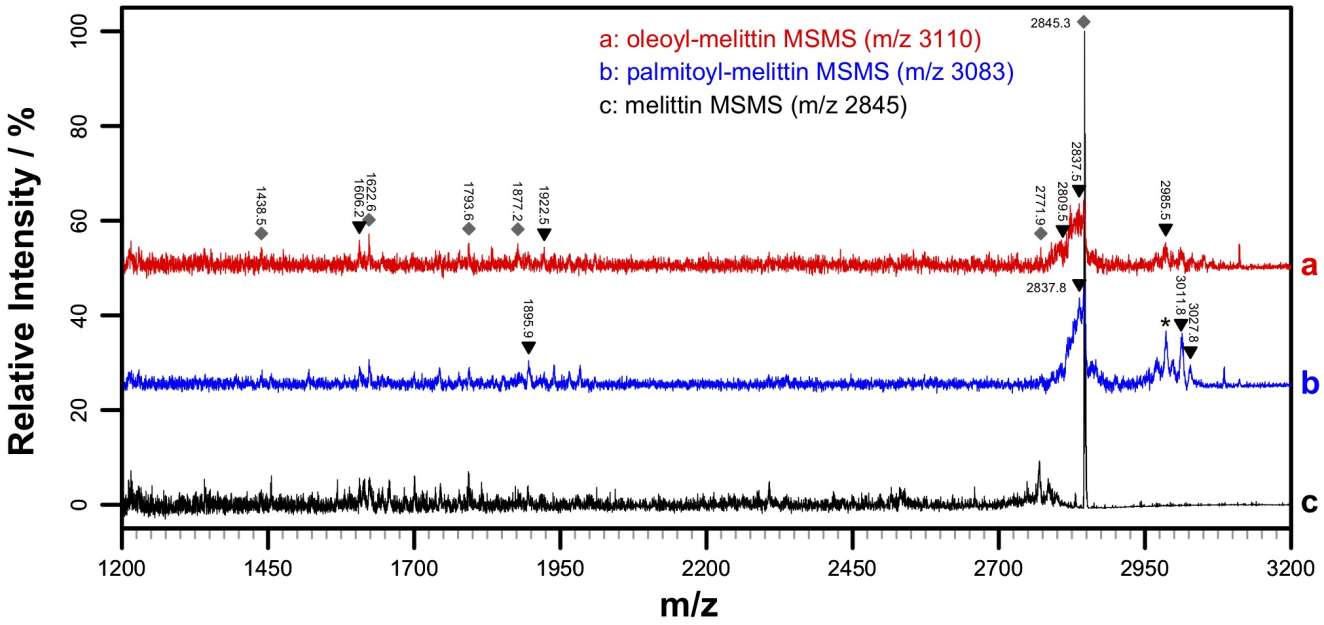

Fig. S9 High mass region of the MS/MS fragmentation spectra of (A) oleoyl-melittin (*m/z* 3110), (B) palmitoyl-melittin (*m/z* 3083) and (C) melittin (*m/z* 2845). Product ions that correpond to potential matches for modified fragments are indicated by triangles. Product ions that correspond to unmodified fragments are indicated by diamonds. Asterisks denote product ions arising from incomplete isolation of the parent ion. For full peak listings *vide infra*.

Obs. *m/z*	Rel. Abund. (%)	Assignment	Calc. *m/z*	Fragment
41.6	9	G	41.0	b-17
58.6	9	G	58.0	b
70.1	12	P	70.1	im
72.2	13	V	72.1	im
74.3	14	T	74.1	im
84.1	24	K	84.1	im
86.1	80	I	86.1	im
		L	86.1	im
112.1	11	R	112.2	im
113.2	12	I	114.1	im
		L	114.1	im
129.1	95	Q	129.1	y-17
		GA	129.1	int
		K	129.1	im
		R	129.1	im
146.3	8	Q	146.1	y
154.1	4	GI	154.1	b-17
159.1	17	TG	159.1	int
		W	159.1	im
169.2	35	PA	169.1	int
171.1	16	GI	171.1	b
		Q	172.1	x
		GI	171.1	int
		IG	171.1	int
		AV	171.1	int
		GL	171.1	int
185.2	17	VL	185.2	int
		AL	185.1	int
200.2	12	GIG	200.1	a
		GAV	200.1	int
		KV	200.2	int
		LI	199.2	int
		IS	201.1	int
211.2	8	GIG	211.1	b-17
		LP	211.1	int
228.2	33	GIG	228.1	b
		GIG	228.1	int
		GAV	228.1	int
		KV	228.2	int
		QQ	229.1	int
242.2	74	IGA	242.2	int
		LK	242.2	int
		IK	242.2	int
257.2	9	QQ	257.1	y-17
		KR	257.2	int
		RK	257.2	int
		RQ	257.2	int
268.3	21	GLP	268.2	int
274.1	21	QQ	274.2	y
		SW	274.1	int
282.1	65	GIGA	282.1	b-17
		LPA	282.2	int
		PAL	282.2	int
299.1	17	GIGA	299.2	b
		ALI	298.2	int
313.1	12	IGAV	313.2	int
		GAVL	313.2	int
		VLK	313.3	int
		LKV	313.3	int
		KVL	313.3	int
341.2	24	G oleoyl	340.3	c
		IGAV	341.2	int
		GAVL	341.2	int
		VLK	341.3	int
		LKV	341.3	int
		KVL	341.3	int
		TGLP	341.2	int
355.3	10	LTTG	355.4	int-18
		TTGL	355.4	int-18
369.2	18	TGLP	369.2	int
381.1	5	GIGAV	381.2	b-17
396.1	21	LPAL	395.3	int
		PALI	395.3	int
398.2	11	GIGAV	398.2	b
		GIGAV	398.2	int
		IKR	398.3	int
413.2	11	RQQ	413.2	y-17
		AVLK	412.3	int
		VLKV	412.3	int
		TGLPA	412.3	int
		KRK	413.3	int
		RKR	413.3	int
		KRQ	413.3	int
424.0	8	GLPAL	424.3	int
430.0	14	RQQ	430.3	y
435.3	14	GI oleoyl	435.4	b
440.0	9	VLKV	440.3	int
		TGLPA	440.3	int
454.2	8	GI oleoyl	453.4	c
		IGAVL	454.3	int
		LKVL	454.3	int
		PALIS	454.3	int
464.1	11	GIG oleoyl	464.4	a
		KV oleoyl	464.4	int
482.1	11	PALIS	482.3	int
492.2	100	GIG oleoyl	492.4	b
		KV oleoyl	492.4	int
511.5	4	GIGAVL	511.3	b
		AVLKV	511.4	int
524.1	7	VLKVL	525.4	int
		TGLPAL	525.3	int
541.0	8	KRQQ	541.3	y-17
		GAVLKV	540.4	int
		TTGLPA	541.3	int
		KRKR	541.4	int
		RKRQ	541.4	int
558.2	12	KRQQ	558.3	y
		VLTTGL	557.4	int
563.2	37	GIGA oleoyl	563.4	b
639.9	5	GIGAVLK	639.4	b
		PALISW	640.4	int
653.0	6	IGAVLKV	653.5	int
		GAVLKVL	653.5	int
		GLPALIS	652.4	int
663.0	7	GIGAV oleoyl	662.5	b
		IKR oleoyl	662.5	int
672.1	6	SWIKR	671.4	int
680.2	9	GIGAV oleoyl	680.5	c
697.1	11	RKRQQ	697.4	y-17
		AVLKVLT	697.5	int
		KRKRQ	697.5	int
		RKRQQ	697.4	int
714.1	13	RKRQQ	714.4	y
		LKVLTTG	713.5	int
		KVLTTGL	713.5	int
		LISWIK	713.5	int
738.0	5	GIGAVLKV	738.5	b
758.4	5	GIGAVL oleoyl	758.5	b-17
808.3	7	KVLTT oleoyl	807.6	int
825.1	10	KRKRQQ	825.5	y-17
843.3	9	KRKRQQ	842.5	y
888.7	4	AVLKVL oleoyl	888.7	int
939.3	8	IKRKRQQ	938.6	y-17
		LTTGLPALIS	939.6	int
		TGLPALISW	939.5	int
		IKRKRQQ	938.6	int
955.4	9	IKRKRQQ	955.6	y
		SWIKRKR	955.6	int
1003.3	5	GIGAVLKV oleoyl	1002.7	b
1069.5	7	GIGAVLKVL oleoyl	1069.8	a-18
		ALISWIKRK	1068.7	int
		ISWIKRKR	1068.7	int
1115.2	6	GIGAVLKVL oleoyl	1115.8	b
1128.5	8	GIGAVLKVLTTG	1128.7	c
1142.6	11	WIKRKRQQ	1141.7	y
1156.4	23	unk	unk	unk
1178.5	5	GIGAVLKVLTTGL	1178.8	a-17
		VLKVLTTGLPAL	1178.8	int
		LPALISWIKR	1178.7	int
1438.5	4	LISWIKRKRQQ	1437.9	y-17
		TTGLPALISWIKR	1437.9	int
1606.2	6	PALISWIKRKRQQ	1606.0	y-17
		ISWIKRKRQQ oleoyl	1606.1	y
		LKVLTTGLPALISWI	1607.0	int
1622.7	7	PALISWIKRKRQQ	1623.0	y
		KVLTTGLPALISWIK	1622.0	int
		VLTTGLPALISWIKR	1622.0	int
1793.6	5	GLPALISWIKRKRQQ	1793.1	y
1877.2	5	TGLPALISWIKRKRQQ	1877.1	y-17
		AVLKVLTTGLPALISWIK	1877.2	int
		KVLTTGLPALISWIKRK	1878.2	int
1922.5	4	GIGAVLKVLTTGLPALIS oleoyl	1923.3	a-18
2771.9	4	IGAVLKVLTTGLPALISWIKRKRQQ	2771.7	y-17
2809.5	5	GIGAVLKVLTTGLPALISWIKRKR oleoyl	2808.9	a
2837.5	14	GIGAVLKVLTTGLPALISWIKRKR oleoyl	2836.9	b
		AVLKVLTTGLPALISWIKRKRQQ oleoyl	2837.9	int
2845.7	15	GIGAVLKVLTTGLPALISWIKRKRQQ	2845.8	y
2985.5	5	GIGAVLKVLTTGLPALISWIKRKRQ oleoyl	2984.7	c

Table S1 Peak assignments for fragmentation of oleoyl-melittin (*m/z* 3110). Key: im, immonium ion; int, internal fragment; unk, unknown; a, b, c, b, y: fragment types. All potential matches are shown within an error of ± 1 mass unit.

Obs. *m/z*	Rel. Abund. (%)	Assignment(s)	Calc. *m/z*	Fragment
58.6	7	G	58.0	b
74.9	15	T	74.1	im
86.1	100	I	86.1	im
		L	86.1	im
112.1	11	R	112.2	im
129.1	96	Q	129.1	y-17
		GA	129.1	int
		K	129.1	im
		R	129.1	im
143.2	5	GI	143.1	a
		IG	143.1	int
		AV	143.1	int
		GL	143.1	int
159.1	13	TG	159.1	int
		W	159.1	im
169.1	40	PA	169.1	int
171.1	16	GI	171.1	b
		GI	171.1	int
		IG	171.1	int
		AV	171.1	int
		GL	171.1	int
185.1	12	VL	185.2	int
		AL	185.1	int
200.1	10	GIG	200.1	a
		GAV	200.1	int
		KV	200.2	int
		LI	199.2	int
		IS	201.1	int
213.1	10	VL	213.2	int
228.1	36	GIG	228.1	b
		GAV	228.1	int
		KV	228.2	int
		LI	227.2	int
242.1	68	IGA	242.2	int
		LK	242.2	int
		IK	242.2	int
257.3	6	QQ	257.1	y-17
		KR	257.2	int
		RK	257.2	int
		RQ	257.2	int
268.1	27	G palmitoyl	268.3	a
		GLP	268.2	int
272.1	10	GIGA	271.2	a
		GIGA	271.2	int
		TGL	272.2	int
		WI	272.2	int
274.1	22	QQ	274.2	y
		SW	274.1	int
282.1	63	GIGA	282.1	b-17
		LPA	282.2	int
		PAL	282.2	int
296.1	7	G palmitoyl	296.3	b
299.1	18	GIGA	299.2	b
		ALI	298.2	int
314.0	10	G palmitoyl	314.3	c
		IGAV	313.2	int
		GAVL	313.2	int
		VLK	313.3	int
		LKV	313.3	int
		KVL	313.3	int
		VLT	314.2	int
		LIS	314.2	int
341.1	25	IGAV	341.2	int
		GAVL	341.2	int
		VLK	341.3	int
		LKV	341.3	int
		KVL	341.3	int
		TGLP	341.2	int
369.0	16	GIGAV	370.2	a
		TGLP	369.2	int
395.1	17	LPAL	395.3	int
		PALI	395.3	int
398.1	11	GIGAV	398.2	b
		IKR	398.3	int
409.2	8	GI palmitoyl	409.3	b
412.9	8	RQQ	413.2	y-17
		AVLK	412.3	int
		VLKV	412.3	int
		TGLPA	412.3	int
		KRK	413.3	int
		RKR	413.3	int
		KRQ	413.3	int
424.1	7	GLPAL	423.4	int
430.0	9	RQQ	430.3	y
452.1	9	LK palmitoyl	452.4	int
		GLPAL	452.3	int
		IK palmitoyl	452.4	int
466.2	36	GIG palmitoyl	466.4	b
		GIG palmitoyl	466.4	int
		KV palmitoyl	466.4	int
482.0	11	GIGAVL	483.3	a
		PALIS	482.3	int
492.1	56	GIG oleoyl	492.4	b*
503.7	6	unk	unk	unk
511.1	6	GIGAVL	511.3	b
		AVLKV	511.4	int
537.2	18	GIGA palmitoyl	537.4	b
		GLPALI	537.4	int
541.2	8	KRQQ	541.3	y-17
		GAVLKV	540.4	int
		TTGLPA	541.3	int
		KRKR	541.4	int
		RKRQ	541.4	int
563.1	23	GIGA oleoyl	563.4	b*
558.0	11	KRQQ	558.3	y
		VLTTGL	557.4	int
636.3	4	GIGAV palmitoyl	636.5	b
		IKR palmitoyl	636.5	int
640.1	5	GIGAVLK	639.4	b
		PALISW	640.4	int
680.3	8	GAVLK palmitoyl	679.5	int
		KVLT palmitoyl	680.5	int
		RKR palmitoyl	679.5	int
		GIGAV oleoyl	680.5	c*
697.1	9	RKRQQ	697.4	y-17
		AVLKVLT	697.5	int
		KRKRQ	697.5	int
714.1	18	RKRQQ	714.4	y
		LKVLTTG	713.5	int
		KVLTTGL	713.5	int
		LISWIK	713.5	int
738.9	5	GIGAVLKV	738.5	b
		LTTGLPAL	739.5	int
		TTGLPALI	739.5	int
782.1	5	GAVLKVLT	782.5	int
		KVLTT palmitoyl	781.6	int
		KVLTTGLP	782.5	int
		LPALISW	781.5	int
		PALISWI	781.5	int
		IKRKRQ	782.5	int
808.3	4	KRKR palmitoyl	807.6	int
		RKRQ palmitoyl	807.6	int
		KVLTT oleoyl	807.6	int*
825.2	7	KRKRQQ	825.5	y-17
842.3	10	KRKRQQ	842.5	y
939.4	6	IKRKRQQ	938.6	y-17
		LTTGLPALIS	939.6	int
		TGLPALISW	939.5	int
955.4	11	IKRKRQQ	955.6	y
		SWIKRKR	955.6	int
977.2	5	GIGAVLKV palmitoyl	976.7	b
1128.3	13	GIGAVLKVLTTG	1128.7	c
1141.4	15	WIKRKRQQ	1141.7	y
1150.0	8	GAVLKVLTTGLP palmitoyl	1150.8	int
		LPALISWIKR	1150.7	int
		GAVLKVLTTGLP	1150.7	int
		ISWIKRK palmitoyl	1150.8	int
1156.4	48	unk	unk	unk
1178.6	11	GIGAVLKVLTTGL	1178.8	a-17
		GAVLKVLTTG palmitoyl	1178.8	int
		VLKVLTTGLPAL	1178.8	int
		LTTGLPALIS palmitoyl	1177.8	int
		TGLPALISW palmitoyl	1177.8	int
		LPALISWIKR	1178.7	int
		ALISWIKR palmitoyl	1178.8	int
1895.9	6	GIGAVLKVLTTGLPALIS palmitoyl	1897.3	a-18
		TGLPALISWIKRKRQQ	1894.3	y-17
2837.8	19	AVLKVLTTGLPALISWIKRKRQQ palmitoyl	2838.8	y-18
2845.3	22	GIGAVLKVLTTGLPALISWIKRKRQQ	2845.8	y
3011.8	10	IGAVLKVLTTGLPALISWIKRKRQQ palmitoyl	3010.8	y-17
3027.8	5	IGAVLKVLTTGLPALISWIKRKRQQ palmitoyl	3027.0	y

Table S2 Peak assignments for fragmentation of palmitoyl-melittin (*m/z* 3083). Key: im, immonium ion; int, internal fragment; unk, unknown; a, b, c, b, y: fragment types. Fragments arising from incomplete isolation of the parent ion are marked with an asterisk. All potential matches are shown within an error of ± 1 mass unit.

Notes and references

[a] *University Science Laboratories, Department of Chemistry, South Road, Durham, DH1 3LE, UK. Tel: +44 (0)191 3342107; E-mail: j.m.sanderson@durham.ac.uk*
[b] *University of Warwick, Department of Chemistry, Coventry, CV4 7AL, UK. Tel: +44 (0)24 7652 3234; E-mail: A.Rodger@warwick.ac.uk*

1 Calculated using ProtParam (www.expasy.ch/tools/protparam.html) using a modified extinction coefficient for Trp according to Pace (C. N. Pace, F. Vajdos, L. Fee, G. Grimsley, and T. Gray, *Protein Sci.*, 1995, **11**, 2411).